Automated Determination of Crystal Reflectivity in the X-ray Laboratory

Bradley Wideman
University of Rochester Laboratory for Laser Energetics
2008 High School Summer Research Program

INTRODUCTION

The University of Rochester's OMEGA laser [1] is used to research the conditions necessary for inertial confinement fusion. The OMEGA laser produces hot x-ray emitting plasmas when in operation and measurements of the x-ray emission are used to infer conditions in the plasma. One method of observing x rays produced using the OMEGA laser is diffraction by a crystal. The reflectivity of a crystal must be known to infer the absolute x-ray flux from the source. Examples of inferred absolute x-ray spectra obtained from target experiments on OMEGA are given in reference [2].

Crystals are used to diffract x rays. X-ray photons incident on a crystal are preferentially scattered in directions θ that obey the Bragg equation [3]

$$n\lambda = 2d\sin\theta \tag{1}$$

where n is the order of diffraction, λ is the x-ray wavelength, and d is the crystal spacing. The photon energy and wavelength are related by the Planck equation

$$E = \frac{hc}{\lambda} \tag{2}$$

where E is energy, h is Planck's constant, c is the speed of light and λ is the wavelength.

At specific angles, constructive interference (diffraction) occurs. The numbers of incoming and diffracted x-ray photons are measured at specific angles centered on the diffraction peak. Figure 1 shows the reflectivity of a crystal as a function of angle surrounding the Bragg angle. Typical Bragg diffraction peaks have widths of much less than 0.1º.

X rays are produced in the LLE X-ray Laboratory in the following manner: A filament is heated to a high temperature by an electric current thereby emitting electrons in a process known as thermionic emission [4]. A high voltage supply accelerates electrons from the filament towards a metal target. The electrons strike the metal and decelerate, causing x-ray photons to be emitted. The electrons decelerate by different amounts causing a broadband continuum spectrum of x rays to be emitted. Electrons sometimes collide with electrons that are bound within atoms, knocking the electron into a higher-energy bound state or an unbound state. The electrons return to their previous state, producing sharp x-ray peaks at specific energies[5], since electrons contained within atoms have specific energy states.

These x-ray peaks are useful for diffraction measurements because the x-ray photon energy, a parameter of the Bragg angle, is constant. X rays are collimated to minimize angular dispersion. The collimated beam must have a width less than the width of the crystal. A Lithium-drifted Silicon (Si(Li)) detector[6] is used to count diffracted photons. Stepper-motor-driven stages are used for position control. The reflectivity of a KAP (Potassium Acid Phthalate) crystal is determined in this work from measurements taken in the X-ray Laboratory. Other examples of absolute calibrations determined in the LLE X-ray Laboratory are given in references [7,8].

EXPERIMENTS

In order to measure crystal reflectivity, the following apparatus is used (Fig 2). An x-ray source as previously described is contained within a vacuum system. The x rays exit through a thin beryllium window (8.5 μm thick). The source is collimated by a pair of metal slits. The collimated x rays are incident upon a crystal which is mounted on top of 3 stepper-motor-driven stages. A detector is also attached to the stages. The entire path of the x rays after exiting the vacuum system is contained within a helium-filled bag. A viewing scope is placed behind the crystal for alignment purposes.

(a) X-ray Source

The x-ray source is contained within the vacuum system and consists of a filament and a target. Electrons are ejected from the filament through thermionic emission [4] and are accelerated by a 10 kV voltage. A magnet is used to direct the electrons to the target. The bent path minimizes ion contamination from the tungsten filament. In this case, the electrons are incident on a water-cooled aluminum target, producing both broadband x-ray radiation and an Al Kα peak at 1.486 keV.

(b) Collimation

Two slits are used to collimate the x rays. The angular dispersion of a 2-slit collimator can be calculated using the following equation:

$$\theta = 2\tan^{-1}\left(\frac{d}{x}\right) \tag{3}$$

where d is the width of the slits and x is the distance between them. A 0.003 inch (76.2 μm) by 10 mm slit is placed near the x-ray source. This slit is assembled by gluing 2 thin metal pieces, separated by 0.003 inch shim material, to a circular aperture. A 0.003 inch (76.2 μm) by 4 mm slit is placed 1.67 m from the first slit, just outside the vacuum system. This slit consists of a micrometer set to the correct width. The angular dispersion in the horizontal direction is calculated to be 0.0052.° The exit slit height is restricted to 4 mm by placing lead tape over the micrometer.

(c) Helium Bag

Once x rays exit the vacuum system they must pass through a gas without excessive attenuation. The transmission T of x rays can be calculated by the following equation:

$$T = \exp[-\mu_\rho(E)\rho x] \tag{4}$$

where μ_ρ is the energy-dependent mass absorption coefficient, ρ is the density, and x is the distance. Nitrogen, a major component of air, transmits only 25% of x-ray radiation per centimeter at about 1.5 keV (the energy used in this experiment). Helium transmits 99.7% of x-ray radiation per centimeter at 1.5 keV. Both transmisssions are calculated using tabulated values of μ_ρ given in Henke et al. [9] The x rays must travel about 40 cm outside the vacuum system. Over that distance, nitrogen transmission is essentially zero, while helium transmission is 88.7%. As a consequence, to minimize attenuation, the path of the x rays outside of the vacuum system is contained within a helium-filled bag.

(d) Diffraction

The x rays are diffracted by a potassium acid phthalate (KAP) crystal. This crystal has a 2d spacing of 26.632 Å. [9] The Bragg diffraction angle for the Al Kα peak (at 1.486 keV corresponding to 8.34 Å) is calculated to be 18.25.°

(e) Si(Li) Detector

The Si(Li) detector is used to measure the intensity and energy of the diffracted x rays. The Si(Li) detector must be cooled to 77 K with liquid nitrogen to operate properly. The detector produces a pulse for each x-ray photon that it detects. The height of the pulse is proportional to the energy of the photon. The detector is connected to a multichannel analyzer which records the number of counts per energy interval. See the description of Si(Li) detectors and associated electronics given by Knoll [6]. The detector is effectively 100% efficient for photons transmitted through its entrance window (25.4 μm thick Be). For reflectivity measurements, where the ratio of the number of counts incident to reflected is measured with the same detector, no error is introduced.

(f) Positioning Apparatus

Three stepper-motor-driven stages are used to enable accurate positioning of the crystal and the detector (Fig. 2). The linear stage (motor A) controls the horizontal position of both the Si(Li) detector and the crystal. The rotary stages control the angular position of the Si(Li) detector and the crystal. The stages are arranged on top of each other so that the bottom stage (motor B) rotates both the detector and the crystal while the top stage rotates only the crystal. Rotary stages have a position accuracy of 0.01° per step and the linear stage has an accuracy of 0.0001 inch (2.54 μm) per step. This must be taken into account when performing experiments.

(g) Alignment

Two methods are used to align the three stages. The first method is optical alignment. A viewing scope is positioned along a line containing the x-ray source. The scope is positioned such that light passing through the rear collimation slit can be seen by the viewing scope. The positions of stepper-motor-driven stages are initially aligned by the viewing scope to visually determine when the crystal rotary axis is on a line with the collimator. Alignment is accomplished as follows: First the crystal (motor C) is rotated until it is deemed parallel by viewing through the scope. The linear stage (motor A) is then moved until the crystal edge is centered within the viewing scope. Finally, the detector (motor B) is rotated until it appears centered within the scope. The second method of alignment uses the x-ray detector. Each motor is moved in small increments, and the x-ray count rate is recorded at each location. The correct location for the linear stage (motor A) is the location at which the count rate is one-half the maximum (half of the photons should be blocked by the crystal). The correct locations for the rotary stages are the locations at which the count rate is at a maximum. This method is used for rough initial alignment and later refined during the Bragg angle scan.

(h) Stepper Motor Software

The stepper motors are controlled by programmable controllers with built-in inputs and outputs [10]. These inputs and outputs are connected through use of a patch panel, allowing the motors to communicate with each other. The motor controllers are programmed to make all moves automatically, but the software used to record photon spectra with the Si(Li) detector is separate. Thus the entire process is semi-automatic requiring input from the experimenter. Whenever a spectrum measurement is taken, the motor controllers wait for the user to manually take the measurement and flip a momentary switch to signify completion. The program takes measurements of the spectrum at specific angles centered on the predicted location of the Bragg peak. Spectral measurements are also taken of the non-diffracted x-ray beam at the beginning, middle, and end of the diffraction measurements. The actual program instructions are listed in the Appendix.

(i) Measurements

X-ray spectra are measured over a range of angular positions surrounding the nominal Bragg angle. A spectrum consists of the number of photons that are detected at various photon energies during a period of 30 seconds. The undiffracted beam spectrum is captured with the crystal moved out of the x-ray path (Fig. 3). Spectra are taken with the crystal at 0.02° steps ±0.2° from the Bragg angle (Fig. 4). Each spectrum is saved to a file using the ORTEC Maestro [11] multichannel analyzer software, for later processing.

Measurements are taken in a specific order. First, the undiffracted beam is measured, followed by the first half of the Bragg angle scan. Then, the undiffracted beam is measured again, followed by the second half of the Bragg angle scan. A third and final undiffracted beam measurement is made to complete the measurements.

RESULTS

The integrated reflectivity of a crystal is calculated using the recorded spectra. The results are shown in table 1. The integrated reflectivity is initially calculated in the following manner. The integral number of counts of every spectrum is determined in the region containing the Al Kα line. This is shown in the second column of Table 1. The energy range is chosen such that as much as possible of the Al Kα is included, but as little noise and non-Al Kα is included as possible. The integrals of the undiffracted spectra varied significantly over time. Because of this the reference integrals are fitted to a parabola to model the change over time. (Fig. 5) The reflectivity can be calculated at each angular position by dividing the counts at that position by the computed undiffracted counts at that time. The reflectivity as a function of angle determined by this method is given in Table 1 column 4. The integrated reflectivity is calculated by summing the measured reflectivities and multiplying by the step size (0.349 milliradians). The integrated reflectivity is found to be 0.0798 milliradians.

In order to refine the calculation of the integrated reflectivity, the spectra are fitted to a Gaussian

$$f(x) = \frac{1}{\sqrt{2\pi\sigma^2}} \exp\left(\frac{-(x-\mu)^2}{2\sigma^2}\right) \tag{5}$$

where x is the angular position, μ is the mean, and σ is the standard deviation. The NLINLSQ routine [12] is used to fit the data to the sum of a Gaussian distribution and a quadratic. Figure 6 shows an example fit to the Al Kα line and a quadratic representing non-Al Kα counts of the undiffracted beam while Figure 7 shows an example fit to a diffracted spectrum. The integral is taken only of the Gaussian, eliminating contributions due to electronic noise and broad-band (continuum) radiation. The Gaussian integral of each spectrum is given in Table 1 column 3. The integrated reflectivity is determined from the ratio of these revised values. The resulting reflectivities are given in Table 1 column 5 and are plotted as a function of angle from the Bragg peak in Figure 8. The revised integrated reflectivity is calculated to be 0.0878 milliradians. The error in this value is determined from the variation of the reflectivity at the peak of the diffraction scan determined from two repeated measurements. A 17% variation is noted resulting in an uncertainty in the integrated reflectivity of ±0.015 milliradians.

The revised method for calculating the integrated reflectivity has a larger value due to the removal of continuum background from the undiffracted spectrum. The diffracted peaks contain little background noise and only decrease slightly when background is removed from the integrals. This results in a higher value for the integrated reflectivity.

In Figure 9, the integrated reflectivity of the KAP crystal at 1.48 keV is compared to two KAP integrated reflectivity graphs given in Henke et al [9]. Figure 9 shows two theoretical models of the KAP crystal, the mosaic and the perfect. All real crystals should have an integrated reflectivity between the theoretical models. The integrated reflectivity of the KAP crystal determined in this work compares favorably with previously determined values shown as black symbols in Figure 9.

CONCLUSIONS

The integrated reflectivity of a KAP crystal has been measured and compared to published values. This data can be used as a basis for further work with the crystal. Stepper motor controllers have been programmed to automate the stepper motor motion and reduce the amount of human input required to measure x-ray diffraction. This program can be used to simplify future experiments and can also be used as a basis for additional automation.

ACKNOWLEDGEMENTS

I would like to thank all of the LLE staff for their generous support. I would specifically like to thank Dr. Frederic J. Marshall for helping me to complete my research, and Dr. Stephen Craxton for giving me the opportunity to participate in this research.

REFERENCES

1. T. R. Boehly, D. L. Brown, R. S. Craxton et al., Opt. Commun. 133, 495 (1997).

2. B. Yaakobi et al., Phys. Plasmas. 4, 3021 (1997).

3. B. D. Cullity, S. R. Stock. Elements of X-ray Diffraction, Third Edition. (Prentice Hall, Inc., Upper Saddle River, NJ, 2001), pp.89-96.

4. B. D. Cullity, S. R. Stock. ibid pp.19-26.

5. B. D. Cullity, S. R. Stock. ibid pp.7-11.

6. Knoll, Glenn F. Radiation Detection and Measurement. (John Wiley & Sons, Inc., New York, 2000) pp. 457-476.

7. F. J. Marshall et al., Rev. Sci. Instrum. 77, 10F308 (2006).

8. F. J. Marshall, J. A. Oertel. Rev. Sci. Instrum. 68, 735 (1997).

9. B. L. Henke, E. M. Gullikson, J. C. Davis. Atomic Data and Nuclear Data Tables. 54, 181-342 (1993).

10. IM483I built by Intelligent Motion Systems, Inc. Taftville, CT 06380.

11. Applied Measurement Technology, ORTEC. Oak Ridge, TN 37831.

12. Visual Numerics, Inc. Houston, Texas 77042.

APPENDIX

This appendix describes the stepper motor program that is used for the diffraction measurements.

Inputs / Output Patch Panel:

A OUT 3 → B IN 2
B OUT 3 → C IN 2
B OUT 1 → A IN 1

Program Operation:

Action to perform	Switch to flip after action has been completed
	GO c, b, a
Take Beam Measurement	Return a
Take Diffraction Measurement	Return b
Take Diffraction Measurement	Return b
…	
Take Diffraction Measurement	Return b
Take Beam Measurement	Return c, b, a
Take Diffraction Measurement	Return b
Take Diffraction Measurement	Return b
…	
Take Diffraction Measurement	Return b
Take Beam Measurement	Return a

Motor Controller A Code:

	Instruction	Comment
0	`-400.`	Moves crystal out of path so a beam measurement can be taken
5	`W0`	Wait for move to complete
8	`L2048 5`	Waits for return switch; a beam measurement is taken at this time.
12	`+400.`	Returns crystal to original location
17	`W0`	Wait for move to complete
20	`A32`	Tells controller b to begin sweep by sending a 100ms high pulse from controller a out 3 to controller b in 2.
22	`W10`	
25	`A0`	
27	`L2048 0`	Waits for a high on input 1; this signifies that controller b is done with the sweep.
31	`J0 2`	Runs the entire program 2 more times: 1 for the 2^{nd} sweep and 1 only for the final beam measurement.
35	`P`	End of Program

Motor Controller B Code:

NOTE: Figure A-1 is a flowchart describing the operation of lines 0-16.

	Instruction	Comment
0	`L19 3`	If input 2 is high jump to line 19. This occurs when controller a signals that the beam measurement is complete and a sweep should begin.
4	`L0 5`	If return switch is flipped continue, else go back to the beginning. If the return switch is flipped at this point it signals the program that this is the 2^{nd} time it is being run and it should move an additional distance so that the 2^{nd} sweep starts where the 1^{st} sweep left off.
8	`+40.`	This is the extra move that occurs only before the 2^{nd} sweep.
13	`W20`	Waits 200 ms to prevent accidental repetition.
16	`G0`	Returns to beginning.
19	`+3600.`	Begins sweep by moving into position for the 1^{st} measurement.
24	`A32`	Sends a 100 ms high pulse to controller c.
26	`W10`	This tells c to do whatever b just did.
29	`A0`	
31	`W100`	Waits 1 sec to prevent accidental repetition.
34	`L2048 5`	Waits for return switch. This signifies that the spectrum has been recorded.
38	`+4.`	Moves the motor a small amount so that the next measurement can be taken.
43	`j24 9`	Repeats lines 24-38 9 more times (for a total of 10) This allows 11 measurements to be taken.
47	`W100`	Waits 1 sec to prevent accidental repetition.
50	`A32`	Sends a 100 ms high pulse to controller c.
52	`W10`	This tells c to do whatever b just did.
55	`A0`	
57	`L2048 5`	Waits for return switch. This signifies that the final measurement is complete.
61	`A32`	
63	`W10`	Sends a 100ms high pulse to controllers a and c.
66	`A8`	This tells controller a that the sweep is complete.
68	`W10`	This tells controller c to return to angle 0.
71	`A0`	
73	`-3640.`	Returns motor to original location.
78	`W0`	Waits for motor to finish moving.
81	`J0 1`	Runs entire program again for 2^{nd} sweep
85	`-40.`	Moves back extra for 2^{nd} sweep only.
90	`P`	End of Program

Motor Controller C Code:

NOTE: Figure A-1 is a flowchart describing the operation of lines 0-16.

	Instruction	Comment
0	`L19 3`	If input 2 is high jump to line 19. This occurs when controller a signals that the beam measurement is complete and a sweep should begin.
4	`L0 5`	If return switch is flipped continue, else go back to the beginning. If the return switch is flipped at this point it signals the program that this is the 2^{nd} time it is being run and it should move an additional distance so that the 2^{nd} sweep starts where the 1^{st} sweep left off.
8	`+40.`	This is the extra move that occurs only before the 2^{nd} sweep.
13	`W20`	Waits 200 ms to prevent accidental repetition.
16	`G0`	Returns to beginning.
19	`+1800.`	Begins sweep by moving into position for the 1^{st} measurement.
24	`W100`	Waits 1 sec to prevent accidental repetition.
27	`L2048 2`	Waits for signal from controller b. This signifies that the spectrum has been recorded.
31	`+2.`	Moves the motor a small amount so that the next measurement can be taken.
36	`W100`	Waits 1 sec to prevent accidental repetition.
39	`j27 9`	Repeats lines 27-36 9 more times (for a total of 10) This allows 11 measurements to be taken.
43	`L2048 2`	Waits for signal from controller b. This signifies that the final spectrum has been recorded.
47	`-1820.`	Returns motor to original location.
52	`W0`	Waits for motor to finish moving.
55	`J0 1`	Runs entire program again for 2^{nd} sweep
59	`-20.`	Moves back extra for 2^{nd} sweep only.
64	`P`	End of Program

Diffracted Spectra

Position (degrees)	Counts		Reflectivity	
	Sum	Fit	Original	Revised
-0.20	23	20	0.0010	0.0010
-0.18	67	90	0.0024	0.0035
-0.16	242	265	0.0072	0.0087
-0.14	446	436	0.0123	0.0132
-0.12	109	133	0.0026	0.0035
-0.10	114	127	0.0025	0.0030
-0.08	156	191	0.0030	0.0040
-0.06	231	261	0.0045	0.0055
-0.04	535	541	0.0091	0.0100
-0.02	2732	2675	0.0432	0.0458
0.00a	6454	6435	0.0986	0.1064
0.00b	9125	9009	0.1268	0.1355
0.02	1207	1189	0.0163	0.0174
0.04	356	376	0.0047	0.0053
0.06	177	226	0.0023	0.0031
0.08	123	139	0.0015	0.0019
0.10	76	84	0.0009	0.0011
0.12	44	75	0.0005	0.0010
0.14	51	75	0.0006	0.0009
0.16	39	60	0.0004	0.0007
0.18	32	11	0.0004	0.0001
0.20	41	60	0.0004	0.0007
Reflectivity Sum			0.2287	0.2514

repeated measurements

Un-diffracted Spectra

Time	Counts	
	Sum	Fit
11:33	16455	14846
11:53	67682	62507
12:08	96083	89039

Table 1 – Summary of experimental measurements.

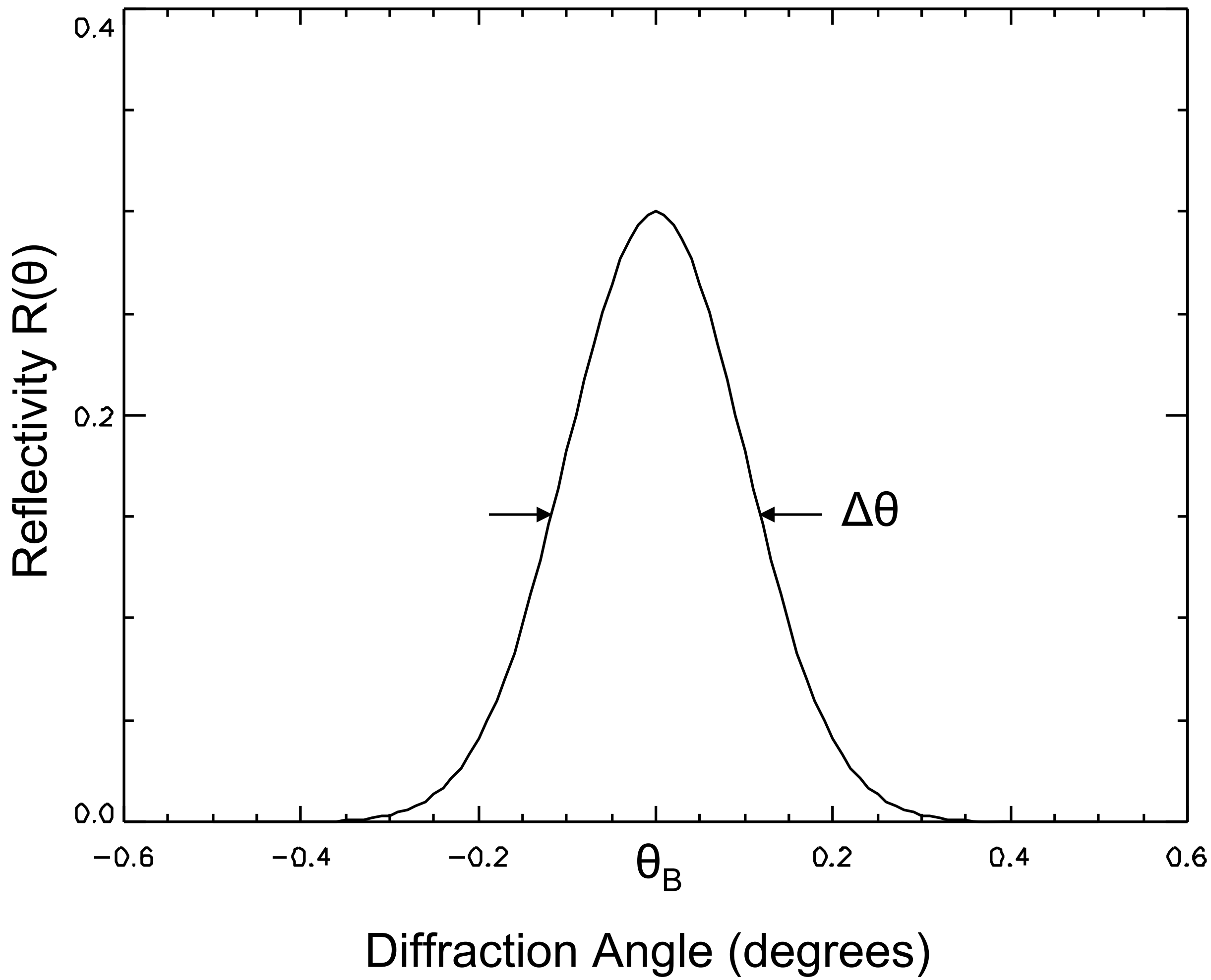

Figure 1 – An idealized example of a Bragg diffraction peak.

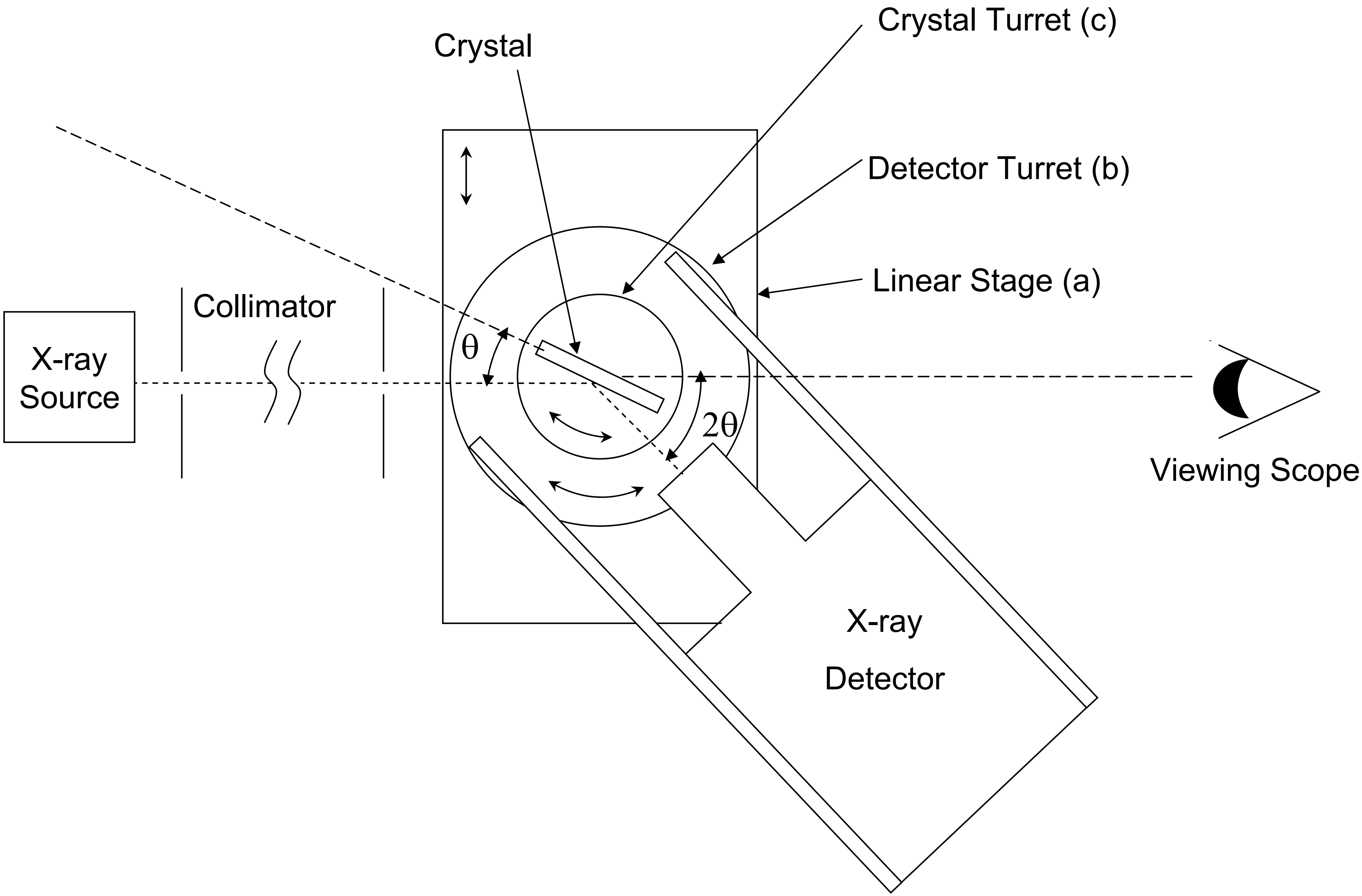

Figure 2 – Diagram of the equipment used for the x-ray diffraction experiment.

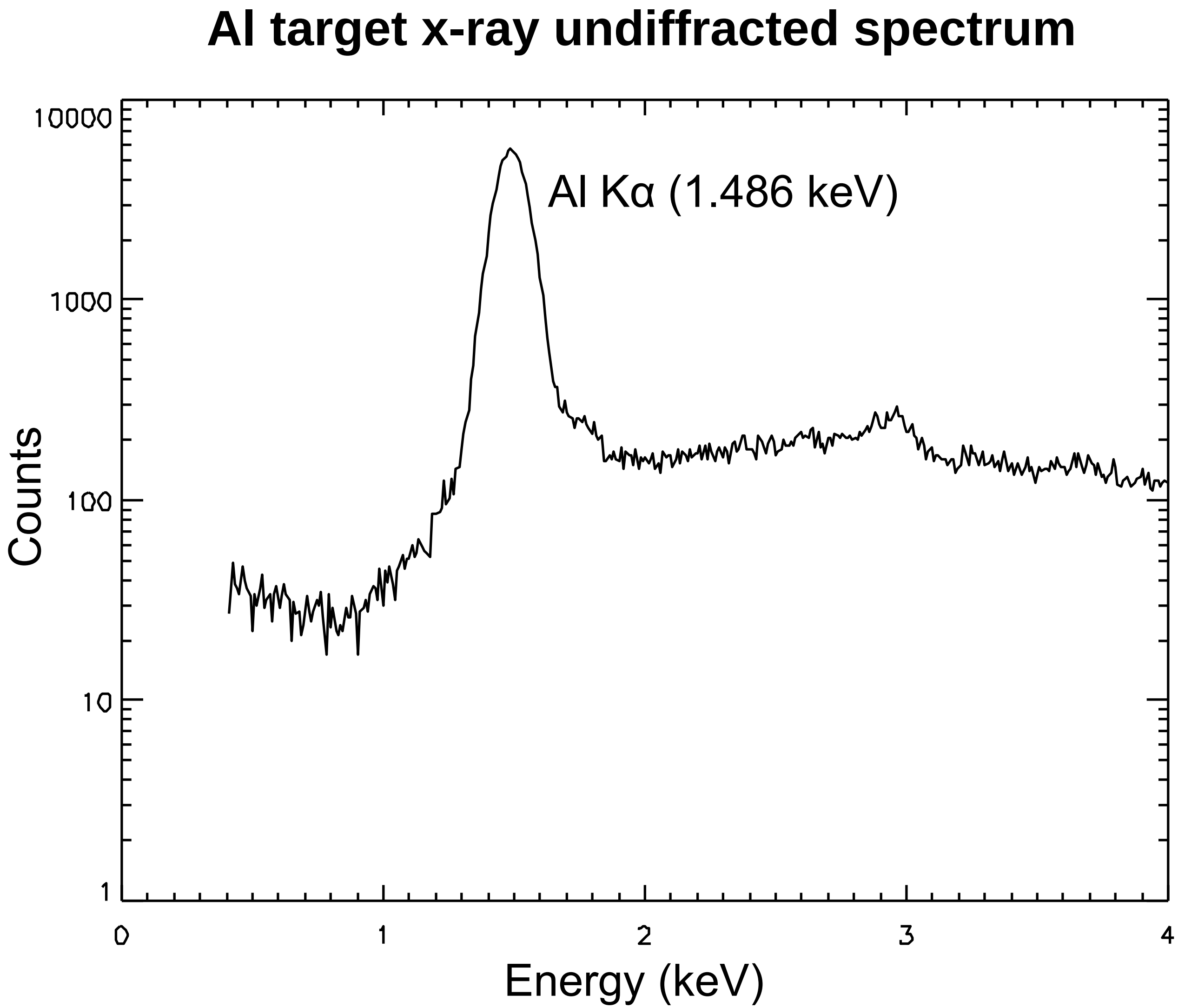

Figure 3 – Spectrum of the undiffracted beam.

Al target x-ray diffracted spectrum at Al Kα peak

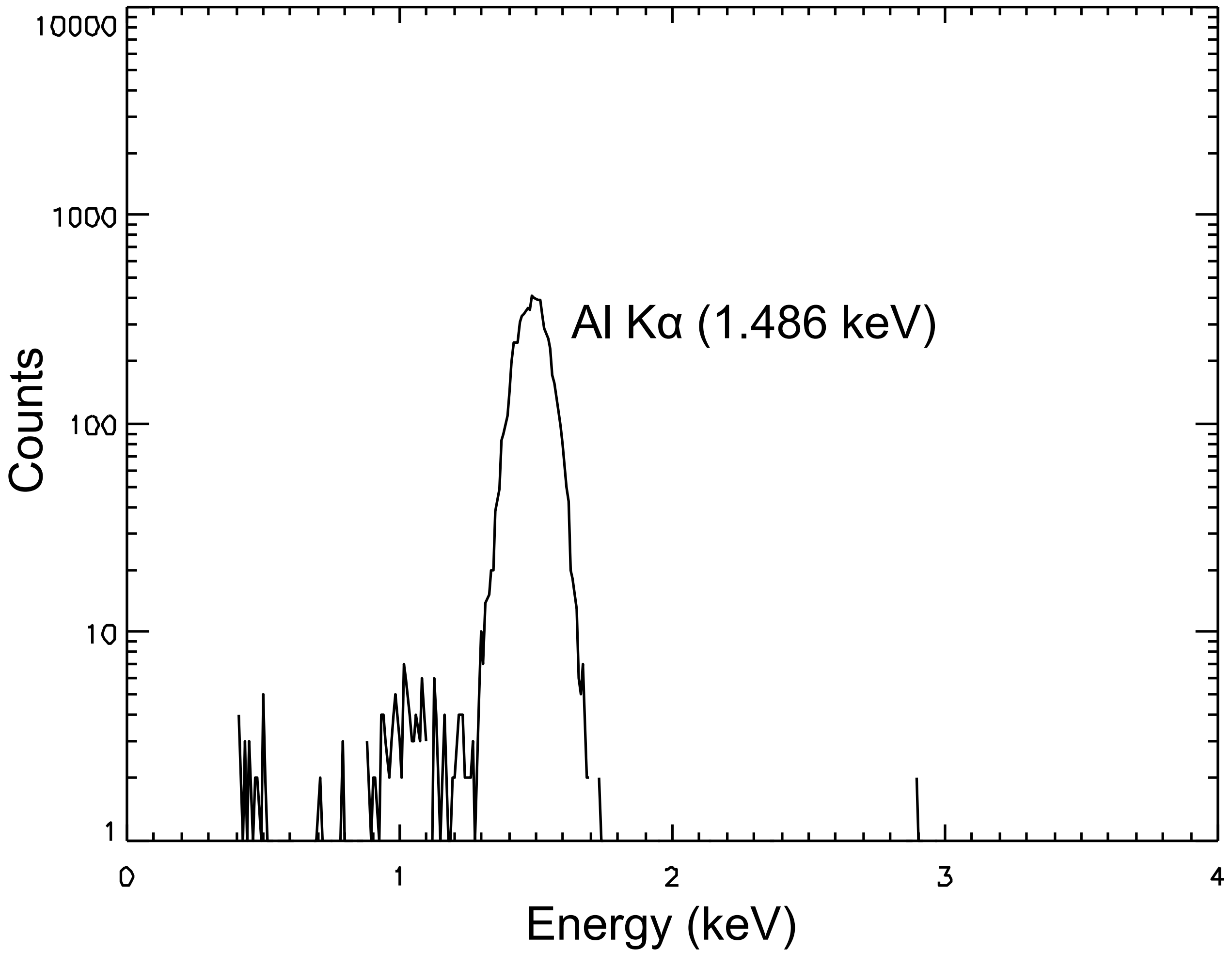

Figure 4 – X-ray spectrum of the KAP diffracted beam.

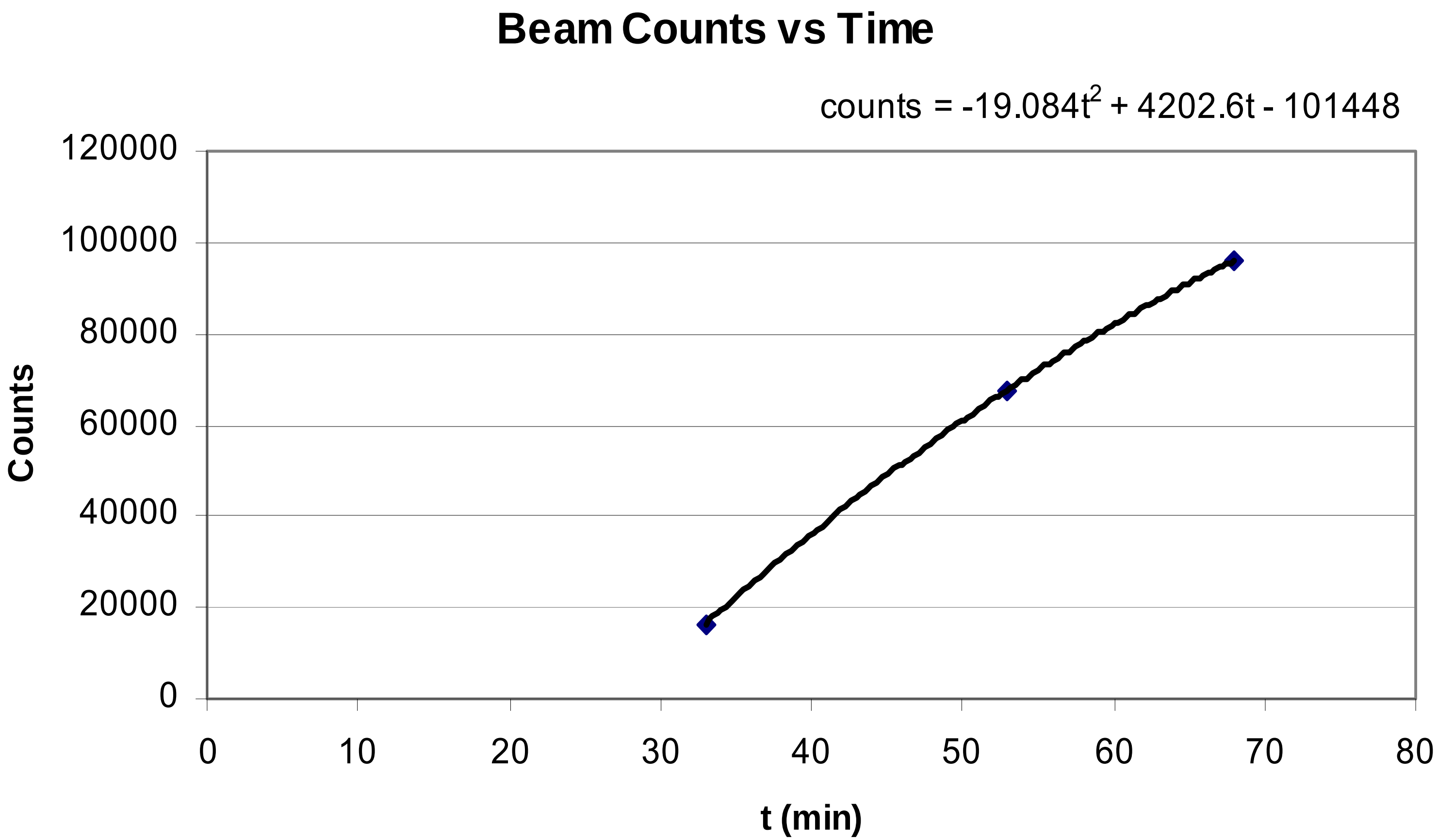

Figure 5 – Undiffracted counts as a function of time.

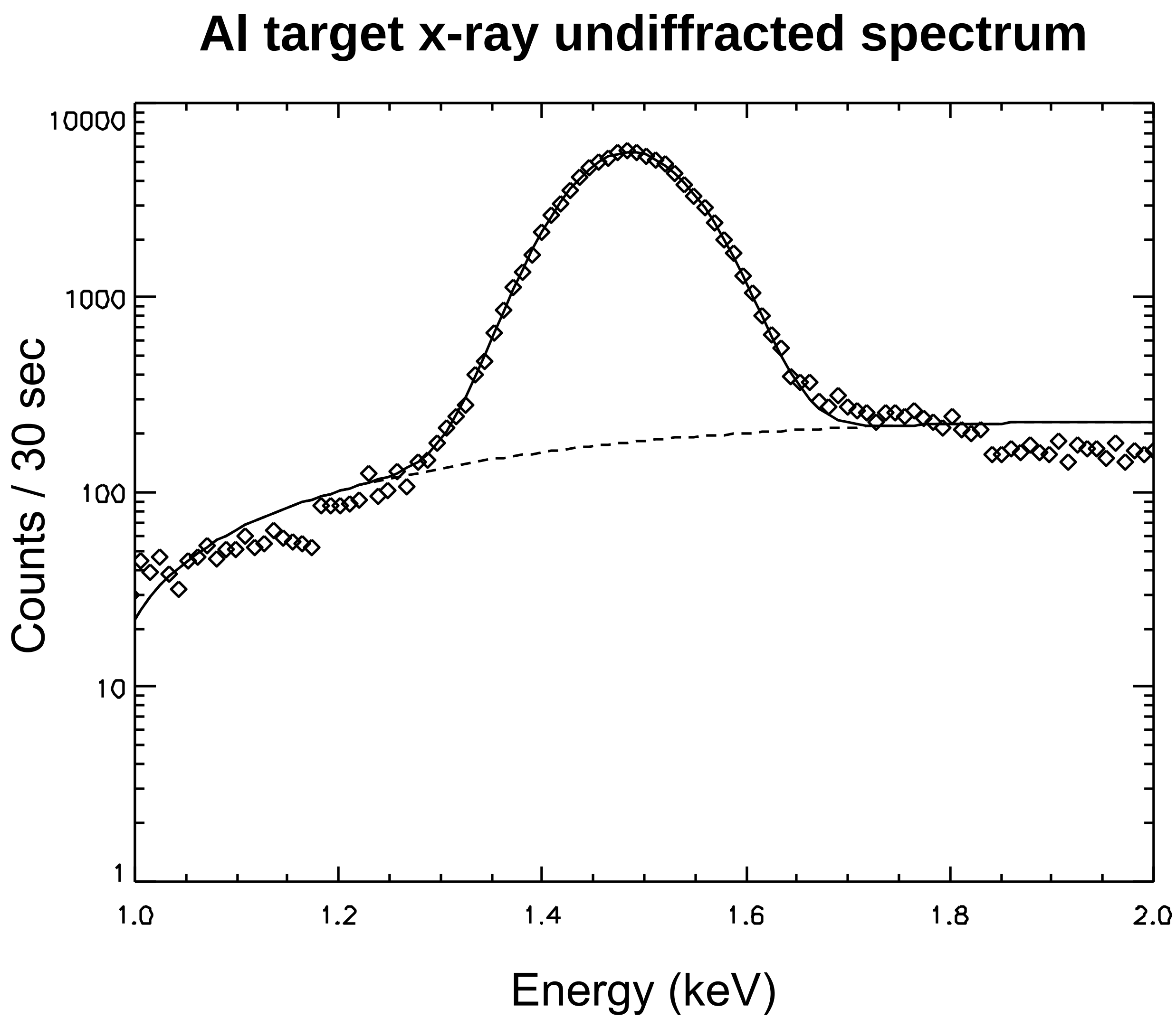

Figure 6 –Gaussian + quadratic fit to the un-diffracted spectrum. The diamonds represent the actual counts observed, the solid line represents the fitted Gaussian, and the dashed line represents quadratic fit to the background.

Al target x-ray diffracted spectrum at Al Kα peak

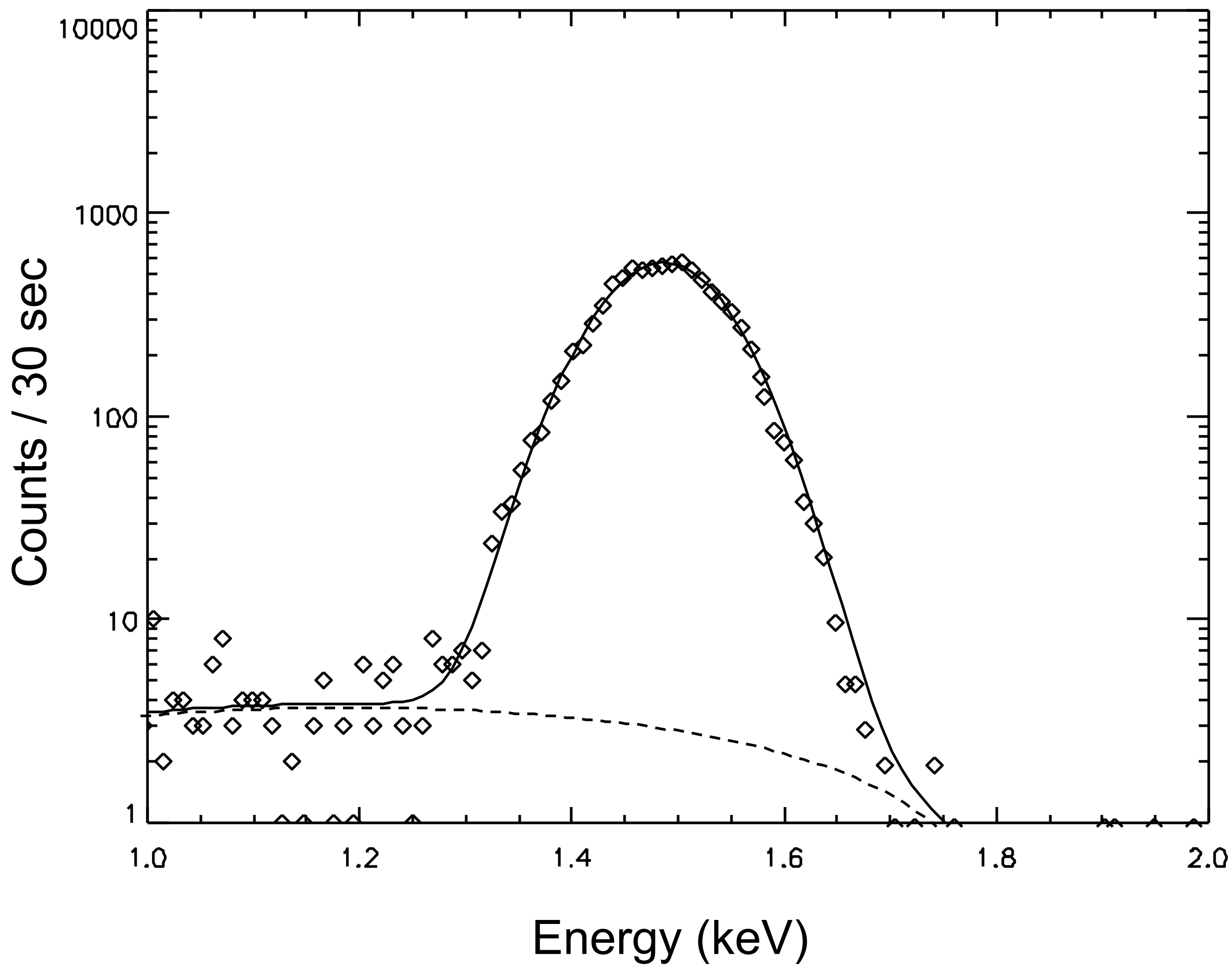

Figure 7 –Gaussian fit + quadratic fit to the diffracted spectrum. See the Figure 6 caption for details.

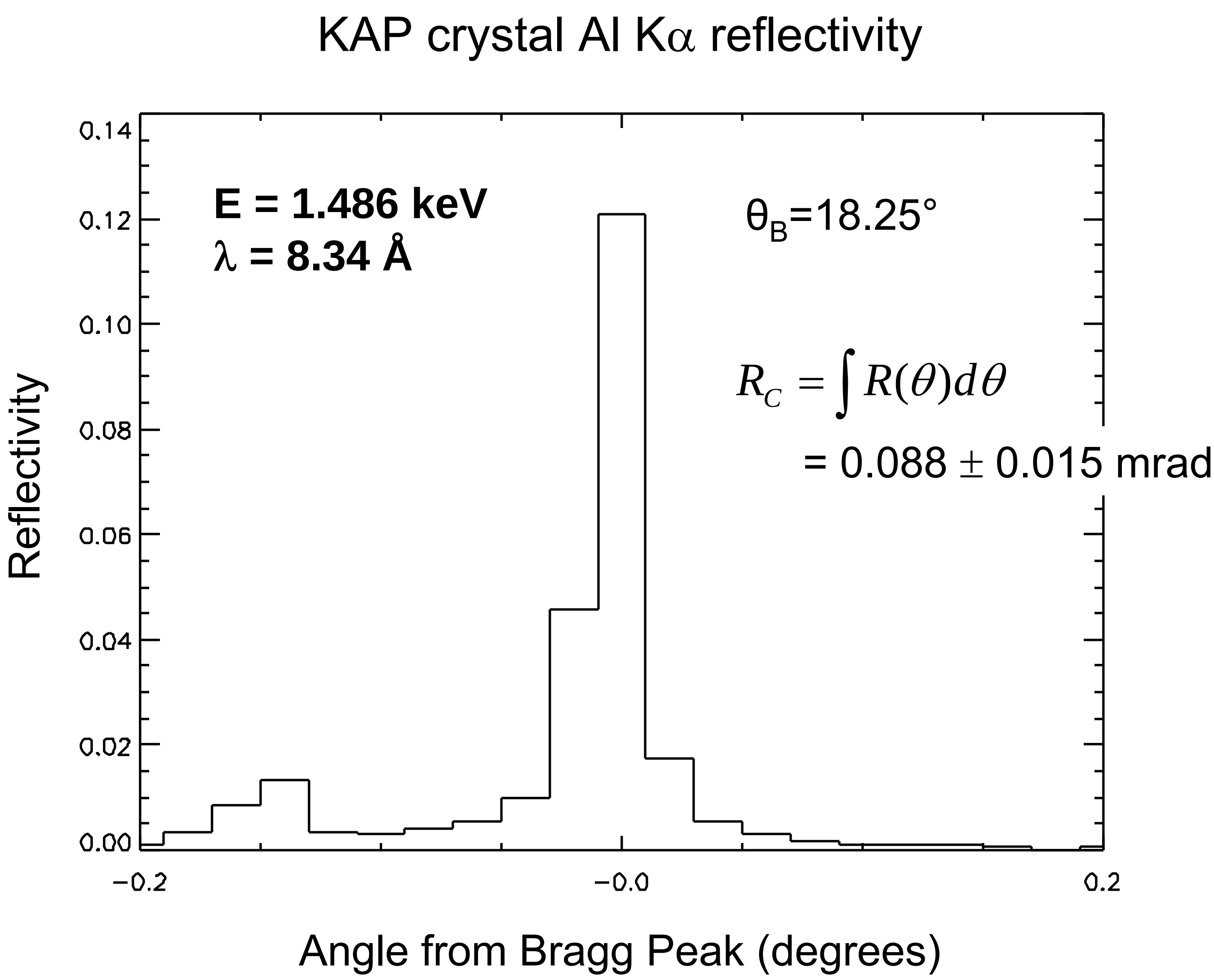

Figure 8 – KAP Crystal Reflectivity as a function of angle from the Bragg peak at 1.486 keV.

KAP crystal integrated reflectivity

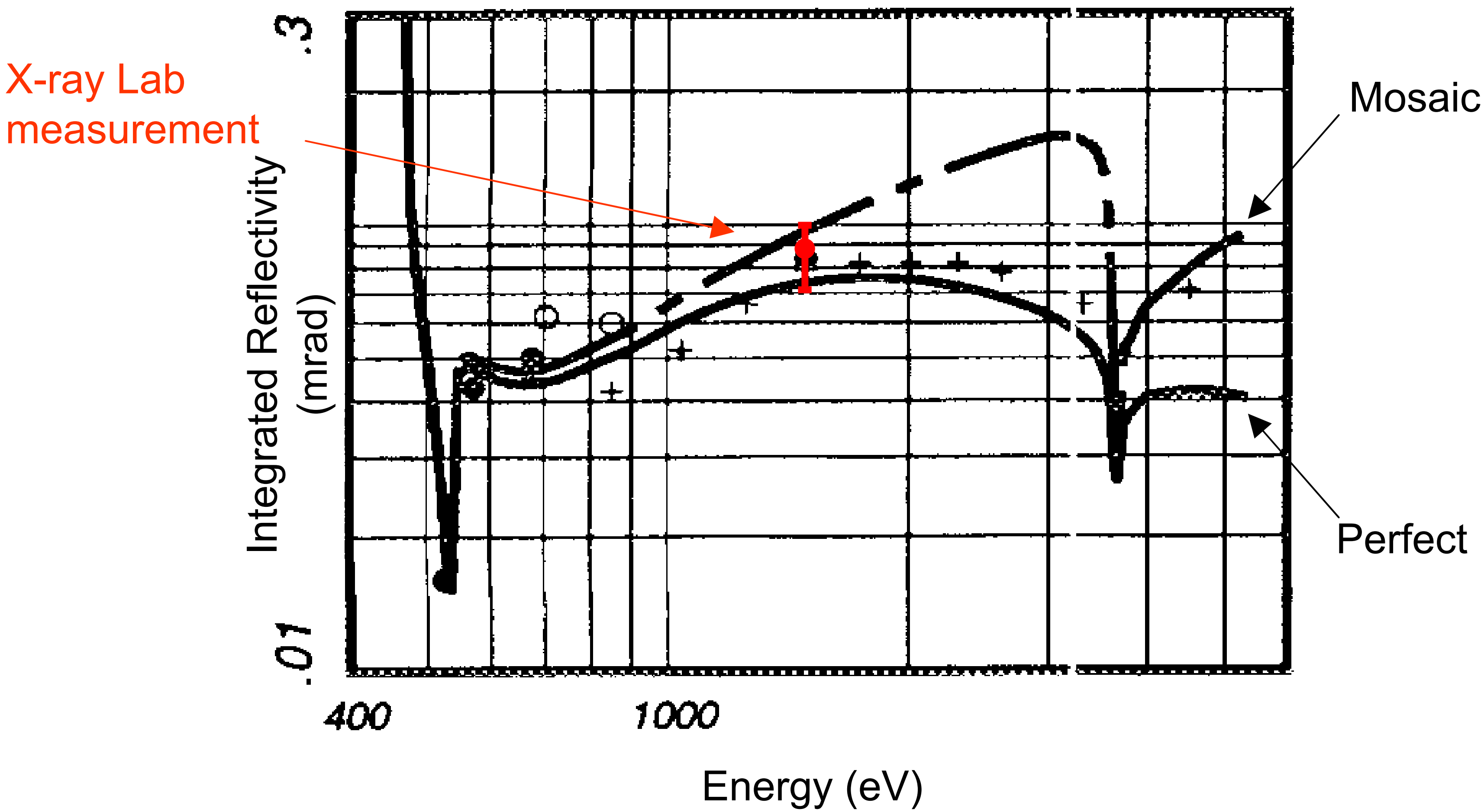

Figure 9 – Graph of KAP crystal integrated reflectivity as a function of energy. Marked in red is the value found in the x-ray laboratory at LLE.

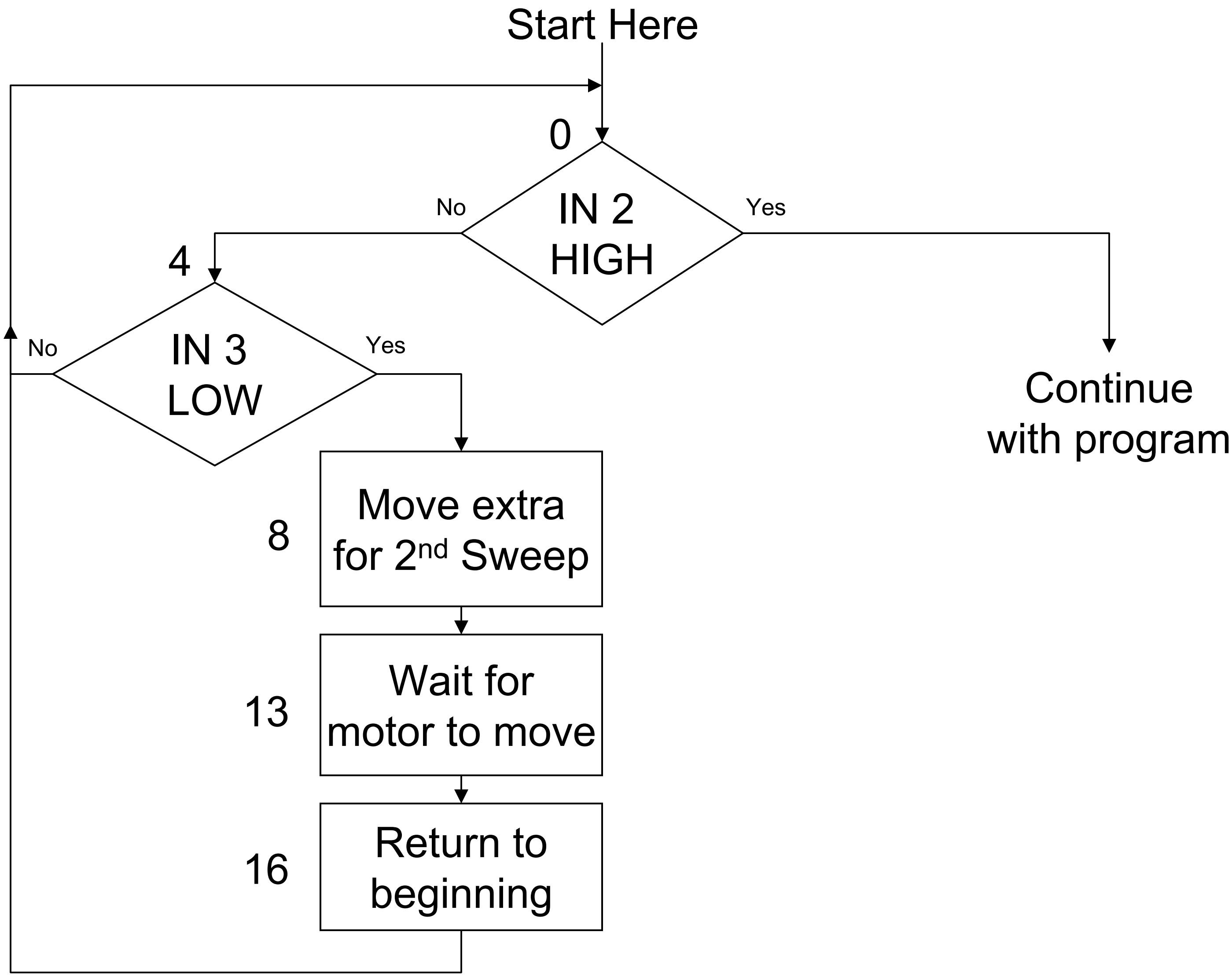

Figure A-1 – A flowchart describing program lines 0-16 on motor controllers b and c.